

Low-energy spectrum and finite temperature properties of quantum rings

P. Koskinen, M. Koskinen, and M. Manninen^a

Department of Physics, University of Jyväskylä, 40321 Jyväskylä, Finland

Received 18 January 2002

Published online 13 August 2002 – © EDP Sciences, Società Italiana di Fisica, Springer-Verlag 2002

Abstract. Recently it was demonstrated that the rotational and vibrational spectra of quantum rings containing few electrons can be described quantitatively by an effective spin-Hamiltonian combined with rigid center-of-mass rotation and internal vibrations of localized electrons. We use this model Hamiltonian to study the quantum rings at finite temperatures and in presence of a nonzero magnetic field. Total spin, angular momentum and pair correlation show similar phase diagram which can be understood with help of the rotational spectrum of the ring.

PACS. 73.21.Hb Quantum wires – 73.21.La Quantum dots – 71.10.Pm Fermions in reduced dimensions

1 Introduction

Nowadays very sophisticated techniques allows one to construct a large variety semiconductor heterostructures, which have turned out to be interesting both theoretically and practically and are often referred as future components of nanoelectronics. One class of structures form quantum dots, or artificial atoms, which have characteristic discrete energy spectrum like atoms (for a review see [1]). The principle of a quantum dot is to confine a bunch of conduction electrons of a semiconductor heterostructure in a small region of space. Usually the electrons are confined from a two-dimensional (2D) gas. Similarly, in a quantum ring the electrons are confined to move in a ring-shaped, circularly symmetric, potential. Lorke *et al.* [2] and Fuhrer *et al.* [3] have shown that rings containing only a few electrons can be studied experimentally.

A ring can be considered to be cut out from a strictly 2D electron gas. However, in the 2D plane the ring will have a finite thickness, being quasi-one-dimensional. Theoretical interest in quantum rings has been concentrated on the possibility of persistent currents [4–10]. Most of the work is based on studying strictly 1D systems using Hubbard-type model Hamiltonians (for a review on 1D systems see Ref. [11]). While these strictly 1D-systems are exactly solvable in some limiting cases and have revealed interesting results for strongly correlated system (*e.g.* Luttinger liquid and charge-spin separation, for a review see Ref. [12]), it is not easy to draw their relation to a realistic quasi-1D ring with long-range Coulomb interactions.

The pioneering work on *ab initio* electronic structure calculations for quasi-1D rings with a few electrons were done by Chakraborty *et al.* [13,14] using configuration interaction (CI) technique. The ‘exact’ many-body wave function of the CI calculation has a circular symmetry and the internal structure is only seen in correlation functions, which reveal the tendency to antiferromagnetic ordering of the electron spins, in agreement with the results of the Hubbard models. The formation of an antiferromagnetic chain of localized electrons is seen more clearly from the results of the the density functional mean field theory which shows the *internal* symmetry of the many-body state [15]. In a many-body formalism the internal antiferromagnetic order has been observed in studying the pair-correlation function [16] and the excitation spectrum [17,18]. Also in the density functional theory the excitation spectrum indicates the existence of antiferromagnetic spin density wave [19]. The study of the excitation spectrum has shown that narrow rings can be accurately described by mapping the exact Hamiltonian to a model of localized electrons [18]. Similar idea have been used earlier for noncircular quantum dots by Jefferson and Häusler [20].

In this paper we will study the quantum mechanics and statistical physics of small quantum rings using the model Hamiltonian suggested earlier [18]. We extend the model for finite magnetic fields and find an interesting variation of the spin-state as a function of the magnetic field. We show that the parameters of the model Hamiltonian are smooth functions of the thickness and radius of the ring. Consequently, the qualitative properties of the ring are insensitive to the parameters of the ring. Due to the exact solution of the model Hamiltonian the statistical physics of the rings can be solved.

^a e-mail: Matti.Manninen@phys.jyu.fi

The organization of the paper is as follows. In Section 2 we will describe the model Hamiltonian and its relation to the exact Hamiltonian, in Section 3 we present results for zero external magnetic field. In Section 4 the rings in the presence of a magnetic field are studied and Section 5 concludes the paper.

2 Theoretical model

The model potential for a quantum ring can be considered to be the parabolic $V(r) = \frac{1}{2}m^*\omega_0(r-R)^2$, where R is the radius of the ring. The parameter ω_0 describes physically the strength of the confining radial potential: The larger ω_0 , the more strictly electrons are confined to the distance R and deviations in the radial direction are small. For a given number of electrons the ring becomes more one-dimensional if either ω_0 or R or both are increased. The normal many-body Hamiltonian if the quantum ring is

$$H = \sum_{i=1}^N \left[-\frac{\hbar^2}{2m^*} \nabla_i^2 + V(r_i) \right] + \sum_{i<j}^N \frac{e^2}{4\pi\epsilon\epsilon_0} \frac{1}{|\mathbf{r}_i - \mathbf{r}_j|}. \quad (1)$$

The eigenstates of (1) were calculated using the configuration-interaction (CI) method in reference [18]. We have extended these calculations for several values of R and ω_0 . In the case of a relative narrow ring we observed earlier [18] that the energy spectrum could be accurately described with a model Hamiltonian consisting of antiferromagnetic Heisenberg term combined with free rotations of the ring and vibrational states of the localized electrons. The effective Hamiltonian of the system can then be written as

$$H_{\text{eff}} = J \sum_{i,j}^N \mathbf{S}_i \cdot \mathbf{S}_j + \frac{\hbar^2}{2I} \mathbf{M}^2 + \sum_a \hbar\omega_a n_a, \quad (2)$$

where the first term is the normal Heisenberg spin-Hamiltonian and the second term describes the rotation of the molecule with moment of inertia I . Note that the rotation axis is fixed. The last term describes the energies of the vibrational excitations of the system, $\hbar\omega_a$ being the energy of the vibrational mode a and n_a the number of quanta associated with that specific vibrational mode. In a narrow ring the vibrational states are clearly separated from the rotational states like in molecules. However, in the case of very shallow rings (and in quantum dots [22]) the vibrational levels are close to the rotational levels and the model Hamiltonian becomes less accurate. Note that the Heisenberg model is a limiting case of many models of strongly correlated 1D-systems [10,11]. Here it can be understood as coming from the tight-binding coupling (see *e.g.* Ref. [21] between the electron localized in ‘pocket states’ [20]).

The eigenstates of the model Hamiltonian (2) can be solved as follows. First, solving the pure Heisenberg model for N localized electrons in a ring is straightforward. The

Table 1. Symmetry properties of all the eigenstates of the Heisenberg model for a ring of six electrons. L_i shows the angular momenta which the state can get in vibrational mode i ($i = 0$ is the vibrational ground state). In case of degenerate states C_i shows the *trace* of the rotation operation.

| Energy | Spin | C_2 | C_3 | C_6 | σ_d | σ_v | L_0 | L_1 | L_2 | L_3 |
|--------|------|-------|-------|-------|------------|------------|-------|-------|-------|-------|
| -2.803 | 0 | 1 | 1 | 1 | 1 | 1 | 0 | 1,5 | 2,4 | 3 |
| -2.118 | 1 | -1 | 1 | -1 | -1 | 1 | 3 | 2,4 | 1,5 | 0 |
| -1.500 | 0 | -1 | 1 | -1 | 1 | -1 | 3 | 2,4 | 1,5 | 0 |
| -1.281 | 1 | -2 | -1 | 1 | 0 | 0 | 1,5 | 0,2,4 | 1,3,5 | 2,4 |
| -1.000 | 1 | 2 | -1 | -1 | 0 | 0 | 2,4 | 1,3,5 | 0,2,4 | 1,5 |
| -0.500 | 2 | 1 | 1 | 1 | 1 | 1 | 0 | 1,5 | 2,4 | 3 |
| -0.500 | 0 | 2 | -1 | -1 | 0 | 0 | 2,4 | 1,3,5 | 0,2,4 | 1,5 |
| 0.000 | 2 | -2 | -1 | 1 | 0 | 0 | 1,5 | 0,2,4 | 1,3,5 | 2,4 |
| 0.118 | 1 | -1 | 1 | -1 | -1 | 1 | 3 | 2,4 | 1,5 | 0 |
| 0.500 | 1 | 1 | 1 | 1 | -1 | -1 | 0 | 1,5 | 2,4 | 3 |
| 0.781 | 1 | -2 | -1 | 1 | 0 | 0 | 1,5 | 0,2,4 | 1,3,5 | 2,4 |
| 0.803 | 0 | 1 | 1 | 1 | 1 | 1 | 0 | 1,5 | 2,4 | 3 |
| 1.000 | 2 | 2 | -1 | -1 | 0 | 0 | 2,4 | 1,3,5 | 0,2,4 | 1,5 |
| 1.500 | 3 | -1 | 1 | -1 | -1 | 1 | 3 | 2,4 | 1,5 | 0 |

basis consists of 2^N Fock states $|\phi_i\rangle = |\sigma_1\sigma_2\cdots\sigma_N\rangle$ (N localized spin- $\frac{1}{2}$ electrons have 2^N possible combinations of their spins, $\sigma_i = \uparrow, \downarrow$). By direct diagonalization the solved eigenstates can be chosen to be eigenstates of the Heisenberg Hamiltonian, \mathbf{S}^2 and \mathbf{S}_z .

Obtaining the angular momenta of these states is not that simple, but one can determine them in the following way. The general rotation operator acting on states is of the form $e^{i\theta\mathbf{M}}$, where \mathbf{M} is the angular momentum operator and θ is the rotation angle (with direction). We define the rotation operator R acting on basis states $|\phi_i\rangle$ as $R|\sigma_1\sigma_2\cdots\sigma_N\rangle = |\sigma_N\sigma_1\cdots\sigma_{N-1}\rangle$, so that R is equivalent to a rotation of an angle $\theta = 2\pi/N$. Because $|\Psi_j\rangle = \sum c_i|\phi_i\rangle$, so $e^{i\theta\mathbf{M}}|\Psi_j\rangle = \sum c_i R^n|\phi_i\rangle = \sum c'_i|\phi_i\rangle$, when $\theta = n2\pi/N$. If $|\Psi_j\rangle$ is nondegenerate eigenstate of M , the right hand side becomes $e^{i\frac{2\pi n}{N}M}|\Psi_j\rangle$. In the case of degenerate states (state $|\Psi_j\rangle$ is not an eigenstate of R) one has to inspect the *trace* of R , which will give us the possibility to determine the angular momentum with help of the character table of the C_{Nv} group. Following the preceding method M gets the values $0 \dots N-1$, but the spectrum can be obtained for all possible angular momenta. Because $e^{i\theta M} = e^{i\theta(M+\frac{2\pi n}{N})}$ and $\theta = k2\pi/N$, states with angular momentum $M' = M+nN =, n = \pm 1, \pm 2 \dots$ have similar symmetry properties. Table 1 shows explicitly the symmetry properties of a ring for six electrons.

In reference [18] it was shown that the exact rotational spectrum calculated with the CI method consists of separated vibrational bands each of which having spin structure consistent with the Heisenberg model. The rotational energy increases simply as M^2 . Figure 1 shows two examples of the energy spectra of the model Hamiltonian for six electrons together with the spectrum of the noninteracting electrons in an infinitely narrow ring. (For comparison of the spectra of the model Hamiltonian to those of the true Hamiltonian we refer to our earlier paper [18].) In the lowest panel the separation of the spectrum to rotational and vibrational states is clearly seen. Using the term

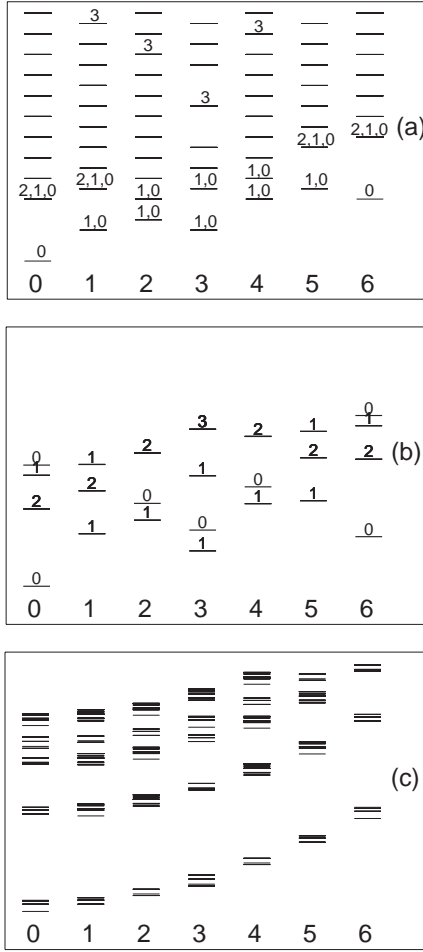


Fig. 1. Energy spectra of six-electron rings for the angular momenta $0 \cdots 6$. The numbers above the energy levels indicate the spin. (a) noninteracting electrons, (b) model Hamiltonian with $IJ = 14$, (c) model Hamiltonian with $IJ = 0.73$. The energy scales are in arbitrary units.

used in nuclear physics we call the lowest energy state for each angular momentum the yrast state, and the lowest vibrational band as yrast band. In the case of six electrons there are only three vibrational modes with energy relations $\omega_1 : \omega_2 : \omega_3 = 1 : \sqrt{7/3} : \sqrt{3}$. The higher vibrational states can be constructed with the help of the yrast band by group-theoretical methods. Table 1 shows how these vibrational states are constructed for the case of six electrons.

The parameters of the model Hamiltonian can be fitted to the results of the exact Hamiltonian. However, knowing that the model Hamiltonian describes narrow quantum rings well, it is interesting to study its properties more systematically in the parameter space determined by J , I , and ω_a at zero and at finite temperatures. Since one of the parameters determines the energy scale and in most cases the vibrational states do not matter (as will be shown below) we have in fact only one parameters $J/(1/I) = IJ$.

The accuracy of the model Hamiltonian depends on the one-dimensionality and on the radius of the ring. The

Table 2. Ratio of the energy differences Δ_6 and Δ_0 (defined in text) calculated with exact diagonalization method. I/I_0 is the ratio of the exact moment of inertia to that of a rigid ring of classical electrons.

| r_s | C_f | Δ_6/Δ_0 | I/I_0 |
|-------|-------|---------------------|---------|
| 2 | 2 | 0.72 | 2.39 |
| 2 | 4 | 0.75 | 1.45 |
| 2 | 10 | 0.88 | 1.03 |
| 2 | 25 | 0.97 | 0.98 |
| 3 | 10 | 0.87 | 1.09 |
| 4 | 10 | 0.87 | 1.14 |
| 4 | 25 | 0.97 | 1.00 |
| 6 | 25 | 0.95 | 1.02 |

one-dimensionality can be expressed in terms of a parameter C_F [22] which is essentially the excitation energy of a radial mode. The ring radius can be related to the one-dimensional density parameter r_s . The resulting relations are $R = Nr_s/\pi$ and $\omega_0 = C_F \hbar^2 \pi^2 / (32mr_s^2)$. The Heisenberg coupling energy of the model Hamiltonian can be fitted to the splitting of the lowest band (vibrational ground state) at a given angular momentum. For example, for six electrons J can be determined from the energy difference of the lowest two $S = 0$, $M = 0$ states, see Figure 1. In the Heisenberg model this energy difference is $3.606J$ as seen from Table 1. Similarly, the moment of inertia can be fitted by requiring that the energy difference between the lowest $M = 6$ and $M = 0$ states is $N/2I$. For narrow rings the fitted moment of inertia is very close to the classical estimate NmR^2 . The accuracy of the model Hamiltonian can then be estimated by studying how well the other energy states are described. The model Hamiltonian predicts that the spectrum for $M = 0$ is identical to that for $M = 6$. In Table 2 we compare the energy difference of the lowest two $S = 0$ states for $M = 6$ (denoted by Δ_6) to that for $M = 0$ (Δ_0). Table 2 also gives the ratio of the moment of inertia determined from the exact spectrum (I) to the classical estimate ($I_0 = NmR^2$). Note however, that the moment of inertia can also be fitted to the exact results. It should be emphasised that using only one parameter all the 23 excited states of the yrast band with their correct spin assignment (shown in Fig. 1b) are reproduced with the model Hamiltonian with the same or better accuracy than the example of the energy ratio shown in Table 2. In the limit of a strictly 1D case ($\omega_0 \rightarrow \infty$) the model Hamiltonian results (numerically) exactly the same spectrum as the true Hamiltonian.

Within the range $2 \leq r_s \leq 6$ and $2 \leq C_F \leq 25$ the product IJ can be accurately described (for six electrons) as

$$IJ = [0.273 + 0.004(r_s^2 C_F) + 2.24 \times 10^{-6}(r_s^2 C_F)^2]^{-1}. \quad (3)$$

In the limit of $r_s \rightarrow 0$ or $C_F \rightarrow 0$ this fit will give $IJ = 3.64$ which is surprisingly close to the similar fit to the noninteracting spectrum, which would give $IJ = 5$.

The effect of a magnetic field \mathbf{B} perpendicular to the plane of the quantum ring can be taken into account

by adding the following terms in the model Hamiltonian (these can be obtained with the normal minimal substitution)

$$\Delta H_B = \frac{e^2}{8mc^2} \mathbf{B}^2 R^2 N + \frac{\hbar e}{2mc} B L_z + g_0 \mu_B B S_z. \quad (4)$$

By considering the magnetic field as a flux penetrating the ring $\phi = \pi R^2 B$ and approximating the moment of inertia by $I = NmR^2$, we get in atomic units

$$H = -J \sum_{i,j} \mathbf{S}_i \cdot \mathbf{S}_j \quad (5)$$

$$+ \frac{1}{R^2} \left[\frac{1}{2N} M^2 + \frac{N}{2} \left(\frac{\phi}{\phi_0} \right)^2 + \left(\frac{\phi}{\phi_0} \right) (M + gS_z) \right], \quad (6)$$

where ϕ_0 is the flux quantum. In addition to the flux ϕ we have (by neglecting the vibrations) only two parameters in the Hamiltonian (6), the Heisenberg coupling J (or $R^2 J$) and the effective Lande factor g .

In a quantum ring the magnetic flux can be constructed using a homogeneous magnetic field, in which case the electron spins also couple with the field ($g = g_0$), or the field can be restricted inside the ring, in which case the electrons are in a zero magnetic field ($g = 0$). Also a partial penetration of the field in the ring region can be described with nonzero g -values. In describing real quantum rings in semiconductors, our parameter g depend thus on the effective Lande factor of the material in question and on the relative strength of the magnetic field on the ring perimeter as compared in the center.

3 Results at zero field

3.1 Hund's first rule

In quantum dots the electronic structure follows the Hund's first rule, that is the spin of the ground state of an open shell is at maximum [23,24]. The same is true also for quantum rings, although in this case the maximum spin can be only $S = 1$ since each shell consists of only two states corresponding to single particle angular momenta m and $-m$. The total spin of the ground state of the Heisenberg Hamiltonian is $S = 0$ for all even number of electrons. However, combined with the rotational states the ground state of the Heisenberg model is not necessarily the ground state of the total Hamiltonian. The lowest $S = 0$ state belongs to the $M = 0$ ground state of the rigid rotation only if $N = 2(2k + 1)$, where k is an integer. In this case the total ground state has $S = 0$. On the other hand, in the case $N = 4k$ the lowest $S = 0$ state of the Heisenberg Hamiltonian belongs to the angular momentum $M = N/2$. Due to the M^2 term in the Hamiltonian the total energy of this state will be pushed higher than the $S = 1$ state belonging to $M = 0$ rotational state. This means that the model Hamiltonian results the

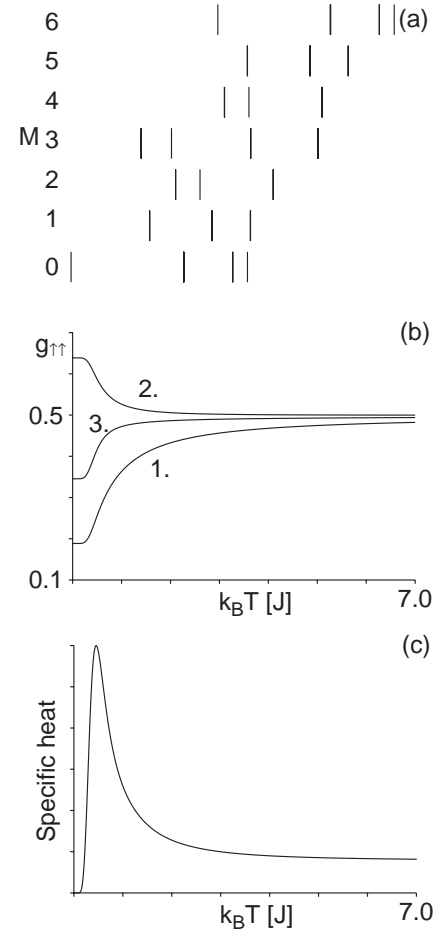


Fig. 2. (a) Energy levels for different angular momentum values (M) in units of J . (b) The pair correlation function at different nearest neighbours (denoted by numbers) as a function of the temperature. (c) The specific heat as a function of the temperature. The ring has six electrons, vibrational states are neglected and $IJ = 6$.

Hund's first rule. (Strictly speaking this requires that IJ is small enough, but, this condition is always valid whenever the model Hamiltonian is a good approximation to the real system.)

3.2 Heat capacity

At finite temperatures the excited states will be populated according to the probabilities determined by the Boltzmann factor. At high temperatures the total spin (the quantum mechanical quantity being S^2) approaches to the average determined by the Heisenberg Hamiltonian, since all states will be populated with equal probability.

The total energy has an expected monotonic behaviour with increasing temperature, but the heat capacity shows a sharp peak at low temperatures due to the discreteness of the energy levels. This is demonstrated in Figure 2 where we show the positions of the energy levels and the heat capacity. Note that the heat capacity peak appears at a much lower temperature than the energy of the first

Table 3. Pair correlation function for the ground state of the six electron ring. For comparison the results of noninteracting tight binding model are shown.

| neighbour | $g_{\uparrow\uparrow}$ | $g_{\uparrow\downarrow}$ | $g_{\uparrow\uparrow}^{TB}$ | $g_{\uparrow\downarrow}^{TB}$ |
|-----------|------------------------|--------------------------|-----------------------------|-------------------------------|
| 1 | 0.189 | 0.810 | 0.278 | 0.500 |
| 2 | 0.638 | 0.362 | 0.500 | 0.500 |
| 3 | 0.346 | 0.654 | 0.444 | 0.500 |

excited state. This, as well as the sharpness of the peak, is caused by the large degeneracy of the first excited state. At higher temperatures the population of the new states increases smoothly and the heat capacity decrease to a constant value. The effect of the vibrational states is only marginal for the for the heat capacity at low temperatures. The reason is that the vibrational states are well separated from the lowest rotational band and a large number of the rotational levels is already populated before the vibrational states start to get marked population.

3.3 Pair correlation function

A natural way to analyse the internal structure of a many-body system is to study the pair correlation function. In the model Hamiltonian the correlation at zero temperature (ground state) arises solely from the Heisenberg model. We define the spin-pair-correlation function as follows:

$$g_{\sigma\sigma'}(d) = \langle \Psi_j | n_{i,\sigma} n_{i+d,\sigma'} | \Psi_j \rangle, \quad (7)$$

where $n_{i,\sigma}$ is the number operator for an electron with spin σ at Heisenberg chain site i . So $g_{\uparrow\uparrow}(d)$ describes the probability for the electron at the site i to have an electron with parallel spin at d th nearest-neighbor site (the spin of the electron at the site i can be either \uparrow or \downarrow) and similarly for opposite spins $g_{\uparrow\downarrow}(d)$. The definition is independent of i by symmetry.

Table 3 gives as an example the pair correlation functions for the six-electron ring. For comparison the correlations for noninteracting electrons in tight binding (TB) model are shown. Incidentally, the correlations of the TB model agree with the values of the pair-correlation function of free electrons in a narrow ring, calculated at angles corresponding to the localized electrons in the TB model. Naturally, the Heisenberg model has a much stronger correlation. In fact the result of the Heisenberg model is in good agreement with the pair-correlation calculated from the exact Hamiltonian in the limit of a narrow ring. Nevertheless, the correlation decreases fast with the distance making the pair correlation function not a clear signature of the particle localization as discussed in reference [18]. In the infinite one-dimensional antiferromagnetic Heisenberg model the pair correlation decreases as $1/d$, d being the distance between the electrons [25].

Figure 2 shows an example of the temperature dependence of $g_{\uparrow\uparrow}(d)$ for different d in the case of a six

electron ring. Figure 2 shows that the antiferromagnetic configuration vanishes essentially at temperatures above the heat capacity peak, *i.e.* at temperatures smaller than the energy of the first excited state. This ‘order-disorder-transition’ is similar to that observed by Borrmann *et al.* [16]. However, Figure 2 shows this behaviour more clearly, because the model Hamiltonian allows us to go to the zero-temperature limit which was not possible using the diffusion Monte Carlo method of reference [16]. Especially, one should note that the strong correlation coming from the ground state can only be seen at very low temperatures and requires that the Monte Carlo method is able to describe the ground state essentially exactly. In the limit $T \rightarrow \infty$ the pair-correlation functions approaches to $\frac{1}{2}$ for all nearest-neighbors, so all spins are oriented at random. Again, the vibrational modes exhibit almost no contribution whatsoever to the pair-correlation functions even with small ω_1 . The reason is that when the vibrational states start to be populated all the possible Heisenberg states of the lowest rotational band are already nearly evenly populated and the correlation has disappeared.

4 Rings at finite magnetic field

A finite magnetic field changes the angular momentum at which the minimum energy is reached and, in the case of nonzero g , splits the degeneracy of different S_z states. Figure 3a shows the phase diagram of S_z for six electrons at zero temperature as a function of magnetic field and g . In the limit of a large field (and nonzero g) the spin is naturally 3, because the energy is minimized by aligning all the spins parallel to the field. On the other hand in the limit of small field, irrespective of g , the spin has the same value as without the magnetic field. As discussed above, for even number of particles this is either 0 or 1 and for odd number of electrons it is $1/2$. Between these extreme limits the spin exhibits interesting *periodic behaviour* as a function of magnetic flux. This is a result of the periodicity of the yrast spectrum (Fig. 1) as a function of M . We can clarify this by writing the relevant terms in (6) as

$$r_0^{-2} \left[\frac{1}{2N} \left(M + \frac{\phi}{\phi_0} N \right)^2 + \frac{\phi}{\phi_0} g_0 S_z \right].$$

Minimizing the energy with specific ϕ means that $M \sim -N\phi/\phi_0$ (M has only discrete values). By increasing ϕ by one flux quantum M decreases by N , giving ultimately the periodicity of ϕ_0 . Depending on J the periodicity can be also ϕ_0/N or $\phi_0/2$. The periodicity ϕ_0/N results if J is so small that all the yrast states for a given M are almost degenerate and, consequently, the energy increases monotonously as a function of M . The periodicity $\phi_0/2$ is seen, when J becomes so large that the yrast states with $L = kN$ and $L = kN + N/2$ are lower in energy than the neighbouring states, see Fig. 1). This behavior is not restricted to rings with six electrons, but is a general property of quantum rings as demonstrated in Figure 3d,

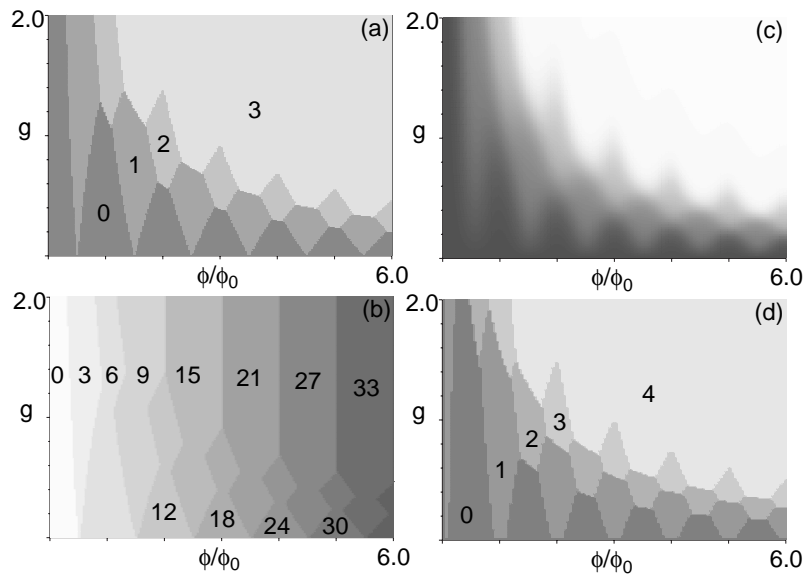


Fig. 3. Total spin (a) and total angular momentum (b) as a function of the magnetic flux and effective Landé factor for a six electron ring ($IJ = 6$). Panel (c) shows the spin at a temperature of $0.5J$. Panel (d) shows the spin for an eight electron ring.

showing the phase diagram for eight electrons. These different periodicities have been observed also using Hubbard models for the quantum ring [10].

The periodicity is shown also in Figure 3b, which represents similar phase diagram for the angular momentum M as a function of magnetic flux and Landé g -factor. Because the state with $S = 3$ has only one angular momentum value in the Heisenberg model (see Tab. 1), Figure 3b shows only angular momentum values $3, 9, \dots$ for large g where the coupling to the spin is strong. When g decreases also other angular momentum values start to exist, corresponding to different spin-values. Notice the resulting similarity of the phase diagrams of S and M in Figures 3a and b.

Figures 3a and d show that the reduction of spin from the maximum value is most easily obtained when the ring is penetrated with an integer number of flux quanta. In this connection it is interesting to note that Maksym and Chakraborty [26] observed similar reduction of the spin from the maximum value at integer numbers of flux quanta for a four electron quantum *dot* using an exact CI calculation for the Hamiltonian (1) with $R = 0$. In the case of four electrons the yrast spectrum of a dot is very similar to that of a ring [22] indicating electron localization. Consequently, the model Hamiltonian gives a simple explanation to this phenomenon observed by Maksym and Chakraborty. The maximum spin belongs to a different angular momentum than the low-spin state and the change of the flux makes the angular momentum to jump with the period $N/2$, until the field is so large that only states with angular momenta with $2, 6, 10, 14$ etc. (for 4 electrons) appear as ground states.

Figure 3c shows the same phase diagram as Figure 3a, but now at the temperature $k_B T = 0.5J$. The periodicity vanishes above temperatures of the order of $k_B T \sim J$. At zero temperature the vibrational states have no meaning

at all, but the remarkable fact is that even at finite temperatures the vibrational states do not have any effect on the phase diagrams, not even even ω_1 as small as $2J$ so that there is no gap between different vibrational bands.

The pair-correlation functions have similar phase diagram as the spin and orbital angular momentum do. For example, the pair-correlation $g_{\uparrow\uparrow}(d) = 1$ for all d , when the spin is three. Decreasing the spin the probability to have opposite spins as nearest neighbors increases with the *same steps* as in the phase diagram for spins.

Let us now consider noninteracting electrons in an infinitely narrow ring. The one-particle states in a one-dimensional ring can be solved easily with periodic boundary conditions. One obtains $\psi(\mathbf{r}) \propto e^{im\phi}$, and the energy $E_m \propto m^2$, where m is the angular momentum for the single-particle states. By setting N electrons in these states according to the Pauli principle, we obtain for the many-particle states $M = \sum_i m_i$, $E = \sum_i \epsilon_i$ and $S_z = \sum_i s_{z,i}$. The many-body spectrum of noninteracting electrons is shown in Figure 1. The yrast states increase roughly as M^2 . The noninteracting spectrum differs in many ways from the spectra of the model (or exact) Hamiltonian shown in Figure 1. For example, it has no different (vibrational) bands but rather a ‘continuum’ of states above the yrast states. Nevertheless, the noninteracting spectrum has a couple of important connection points with the exact spectrum. As discussed above, the ground state for $N = 4k + 2$ has $M = 0$ and $S = 0$, while for $N = 4k$ the $M = 0$ state is degenerate with the $M = N/2$ state, the former having spin 0 or 1 while the latter has spin 0. Moreover, the lowest $S = N/2$ state corresponds to $M = N/2$ in agreement with the results of the model (or exact) Hamiltonian. Consequently, the dependence of the ground state spin as function of the magnetic field and the g parameter is even quantitatively

similar to that of the model Hamiltonian with a suitably chosen coupling constant IJ .

In the limit of the extremely narrow ring, the model Hamiltonian describes not only the lowest rotational band exactly, but also all the vibrational states exactly (without any further parameters) [18]. It seems evident that in this strongly correlated limit the model Hamiltonian becomes an exact description of the true many-body Hamiltonian of interacting electrons. On the other hand many of the results of the model/true Hamiltonian are qualitatively similar to those obtained with the Hubbard-type models with contact interaction between the electrons [9–11]. Further work is needed to find relations between these models.

5 Conclusions

We have studied the magnetization and thermodynamic properties of quasi-one-dimensional quantum rings using a model Hamiltonian previously shown to describe excellently the exact many-body spectra. The properties of the rings are governed by the symmetry of the quantum mechanical system, leading to periodic properties as a function of the magnetic flux. The spin of the ground state has fluctuations obtained earlier using exact diagonalization techniques. Similarly the observed magic angular momentum states which are seen as minima in the yrast line are a natural consequence of the model Hamiltonian.

The temperature dependence of the pair correlation shows that the correlation disappears at low temperatures, corresponding an energy much lower than the lowest electronic excitation of the ring.

A comparison to noninteracting electrons in a narrow ring shows a fundamental similarity which arises of the rotational symmetry and one-dimensionality of the system. The strongly correlated localized electrons result similar phase diagram (spin *versus* magnetic field) to that of noninteracting electrons.

We would like to thank Stephanie Reimann, Susanne Viefers and Prosenjit Singha Deo for several useful discussions. This work has been supported by the Academy of Finland under the Finnish Centre of Excellence Programme 2000-2005 (Project No. 44875, Nuclear and Condensed Matter Programme at JYFL).

References

1. T. Chakraborty, *Quantum dots: A survey of the properties of artificial atoms* (North-Holland, Amsterdam 1999)
2. A. Lorke, R.J. Lyuken, A.O. Govorov, J.P. Kotthaus, J.M. Garcia, P.M. Petroff, Phys. Rev. Lett. **84**, 2223 (2000)
3. A. Fuhrer, S. Lüscher, T. Ihn, T. Heinzl, K. Ensslin, W. Wegscheider, M. Bichler, Nature **413**, 822 (2001)
4. F. Hund, Ann. Phys. (Leipzig) **32**, 102 (1938)
5. M. Büttiker, Y. Imry, R. Landauer, Phys. Lett. A **96**, 365 (1983)
6. L.P. Lévy, G. Dolan, J. Dunsmuir, H. Bouchiat, Phys. Rev. Lett. **64**, 2074 (1990)
7. P. Sandström, I.V. Krive, Ann. Phys. **257**, 18 (1997)
8. S. Viefers, P.S. Deo, S.M. Reimann, M. Manninen, M. Koskinen, Phys. Rev. B **62**, 10668 (2000)
9. F.V. Kusmartsev, J.F. Weisz, R. Kishore, M. Takahashi, Phys. Rev. B **49**, 16234 (1994)
10. F.V. Kusmartsev, Phys. Rev. B **52**, 14445 (1995)
11. E.B. Kolomeisky, J.P. Straley, Rev. Mod. Phys. **68**, 175 (1996)
12. H.J. Schulz, in *Proceedings of Les Houches Summer School LXI*, edited by E. Akkermans, G. Montambaux, J. Pichard, J. Zinn-Justin (Elsevier, Amsterdam, 1995), p. 533
13. T. Chakraborty, P. Pietiläinen, Phys. Rev. B **52**, 1932 (1995)
14. K. Niemelä, P. Pietiläinen, P. Hyvönen, T. Chakraborty, Europhys. Lett. **36**, 533 (1996)
15. S.M. Reimann, M. Koskinen, M. Manninen, Phys. Rev. B **59**, 1613 (1999)
16. P. Borrmann, J. Harting, Phys. Rev. Lett. **86**, 3128 (2001)
17. L. Wendl, V.M. Fomin, A.V. Chaplik, A.O. Govorov, Phys. Rev. A **54**, 4794 (1996)
18. M. Koskinen, M. Manninen, B. Mottelson, S.M. Reimann, Phys. Rev. B **63**, 205323 (2001)
19. A. Emperator, M. Barranco, E. Lipparini, M. Pi, Ll. Serra, Phys. Rev. B **59**, 15301 (1999)
20. J.H. Jefferson, W. Häusler, Phys. Rev. B **54**, 4936 (1996)
21. M.P. Marder, *Condensed Matter Physics* (Wiley, New York 2000)
22. M. Manninen, M. Koskinen, S.M. Reimann, B. Mottelson, Eur. J. Phys. D **16**, 381 (2001)
23. S. Tarucha, D.G. Austing, T. Honda, R.J. van der Haage, L. Kouwenhoven, Phys. Rev. Lett. **77**, 3613 (1996)
24. M. Koskinen, M. Manninen, S.M. Reimann, Phys. Rev. Lett. **79**, 1389 (1997)
25. D. Vollhardt, in *Perspectives in Many-Body Physics*, edited by R.A. Broglia, J.R. Schrieffer, P.F. Bortignon (North-Holland, Amsterdam 1994)
26. P.A. Maksym, T. Chakraborty, Phys. Rev. B **45**, 1947 (1992)